

DRUG DELIVERY STUDY OF SINGLE-WALL CARBON NANOTUBES COVALENT FUNCTIONALIZED WITH CISPLATIN

C. C. CIOBOTARU^{a*}, C. M. DAMIAN^b, S. POLOSAN^a, M. PRODANA^b,
H. IOVU^b

^aNational Institute of Materials Physics, Atomistilor 105 bis, 077125, Magurele,
Bucharest, Romania

^bUniversity POLITEHNICA of Bucharest, Faculty of Applied Chemistry and
Materials Science, Calea Victoriei 149, 010072, Bucharest, Romania

Carbon nanotubes are widely studied components for drug delivery systems due to their high surface area and low chemical reactivity. The research presented in this paper deals with the synthesis of drug delivery systems based on single walled carbon nanotubes (SWCNTs) and the well-known cancer treatment drug Cisplatin. The new nanomaterials obtained through covalent bonding between carboxyl groups from the SWCNTs surface and amino groups from the Cisplatin structure were characterized from structural point of view. To evaluate the content of drug released the Inductively Coupled Plasma Mass Spectrometry (ICP-MS) was employed. The releasing profile shows a slow rate in the beginning followed by a spectacular increase after 180 minutes which means that this type of system could be used for prolonged release.

(Received April 26, 2014; Accepted June 13, 2014)

Keywords: SWCNTs, functionalization, covalent activation, Cisplatin, XPS, ICP-MS

1. Introduction

Nanocarriers for low-molecular-weight drugs offer a promising strategy for improving body distribution and prolonging blood circulation. Recently, single-walled carbon nanotubes (SWCNTs) have been investigated as carriers in living systems [1-4] showing that these materials are very good for drug delivery systems.

Generally, drug delivery systems enter into the cells by endocytosis through the cell membrane. In order to deliver the drugs to the nucleus, it is important that the drug carrier escapes endosomal compartment and releases drug load in cytosolic compartments. One of the advantages of SWCNTs is the capability of delivering chemotherapeutic and imaging agents by overcoming these biological barriers and localizes the target tissue [5-6].

The loaded dose of the drug in direct bonding to CNT is quite limited. Therefore high concentrations of CNT are required for delivery of sufficient amount of drug or the functionalization of CNT. SWCNTs functionalization is important for dispersion and solubilisation [7-8] and to enable further modification [9].

Cis-diammineplatinum(II) dichloride (cisplatin, CDDP) a square planar Pt²⁺ complex was the first metal-based agent which enter into worldwide clinical use for the treatment of cancer. Cisplatin is one of the most potent and widely-used anticancer drug and currently is used either by itself or in combination with other drugs for the treatment of a variety of solid tumors, including testicular, ovarian, bladder, cervical, head and neck, esophageal, colon, gastric, breast, melanoma, prostate cancer, and small-cell lung cancers [10-11].

C. Tripisciano et al. [12] described a method of embedding CDDP through SWCNTs internal diameter. They studied the release of the CDDP bonded noncovalent inside the SWCNTs by ICP showing that 68% of drug was released after 72h.

* Corresponding author: claudiu.ciobotaru@infim.ro

In another study, A. A. Bhirde et al. [13] reported a method of activation of carboxyl functionalized SWCNTs with CDDP by dispersing them in dimethyl sulfoxide at room temperature for 1 h. Using different methods they calculate the size of CDDP molecules bonded on the SWCNTs. Also they observed that one Pt atom is corresponding to 10 nm length of SWCNTs.

K. W. Ciecwierz et al. [14] developed a new method of introducing CDDP inside oxidized SWCNTs by dispersing SWCNTs in a solution of CDDP in dimethylformamide (DMF) or water through sonication followed by stirring for about 20 h at room temperature. After drug release studies they conclude that the best results were obtained using DMF as solvent.

A similar method for encapsulation of CDDP in MWCNT was presented by Li et al [15]. They mixed and ultrasonicated CDDP and MWCNT in ethyl acetate followed by stirring in the dark. They evaluated the loading of CDDP in MWCNTs with TGA and ICP-OES and the result was 0.621 mg of CDDP for each 1 mg of MWCNT-CDDP sample.

The aim of this paper is focused on developing of a new route for synthesis of nanocomposites based on covalent functionalization of SWCNTs with CDDP for drug delivery systems. Several experimental techniques were involved in order to investigate the formation of covalent bonds between SWCNTs and CDDP like Fourier Transform Infrared (FT-IR), Raman Spectroscopy measurements, X-ray Photoelectron Spectroscopy (XPS) and X-ray Diffraction (XRD) for structural characterization. Thermogravimetric Analysis (TGA) and Scanning Electron Microscopy (SEM) were employed to bring additional information about the newly synthesized system. Moreover, Inductively Coupled Plasma Mass Spectrometry (ICP-MS) was used to determine the concentration of drug released.

2. Materials and methods

2.1 Materials

Single-wall carbon nanotubes (SWCNTs) were purchased from Sigma Aldrich having chirality 6,5, more than 90% carbon basis, more than 77% carbon as SWCNTs, and diameter range between 0.7 and 0.9, produced by CoMoCAT[®] Catalytic Chemical Vapor Deposition (CVD) Method.

Activation process was done by using 1-(3-Dimethylaminopropyl)-3-ethylcarbodiimide (EDC), N-Hydroxysuccinimide (NHS) and Cisplatin purchased from Sigma Aldrich.

The reaction was made in potassium phosphate monobasic solution having pH=4.5.

Cellulose dialysis sacks having a molecular weight cutoff of 12000 (Aldrich) were used for the drug release study.

Phosphate buffer solution (PBS) having pH=7.4 was obtained by mixing 250 mL of potassium phosphate monobasic having concentration of 2M and 393.4 mL of sodium hydroxide having concentration of 0.1 M.

2.2 Methods

2.2.1. Activation of SWCNTs purified for 48h and oxidized (SWCNTs-p48h-COOH) with CDDP

SWCNTs as-received were previously purified and oxidized as already described [16]. Covalent functionalization of SWCNTs-p48h-COOH with CDDP was done by using EDC and NHS. Briefly 30 mg of EDC were dissolved in 3ml of phosphate monobasic solution. After that, 30 mg of SWCNTs-p48h-COOH were added. Then 90 mg of NHS were added and the mixture was sonicated 30 min at room temperature (~25°C) for activation of the carboxylic groups. The second step was the addition of 30 mg CDDP to obtain amide bonding to the SWCNTs surface, this step required sonication for another 90 min maintaining the mixture at room temperature. When the sonication was finished the solution was filtered and washed several times with distilled water. The water used for washing was collected and analyzed by ICP-MS in order to calculate the amount of CDDP covalently bonded on the SWCNTs surface using equation (1).

$$CDDP - \text{Loading efficiency \%} = 100 * \frac{(W_{\text{feed}}^{CDDP} - W_{\text{free}}^{CDDP})}{W_{\text{feed}}^{CDDP}} = 100 \quad (1)$$

where W_{feed}^{CDDP} is the mass of CDDP that was introduced into the reaction and W_{free}^{CDDP} is the mass of unbound CDDP that was calculated using ICP-MS from washing solution.

2.2.2. *In vitro* CDDP release covalently bonded onto SWCNTs-p48h-COOH surface.

After activation the SWCNTs with CDDP was dispersed in 5 ml of PBS pH=7.4 for 2 min using ultrasounds for a better dispersion. Then the solution was transferred into a dialysis sack previously washed with PBS 7.4 to remove all the impurities.

The sack containing the solution of SWCNTs with CDDP and PBS was closed to both ends and immersed in a glass with 50 ml of PBS 7.4 and placed on a magnetic stirrer thermostated at 37 °C and 300 rpm. From time to time 4 ml of dissolution medium were extracted and analyzed with ICP-MS. The sample volume was replaced with fresh PBS 7.4

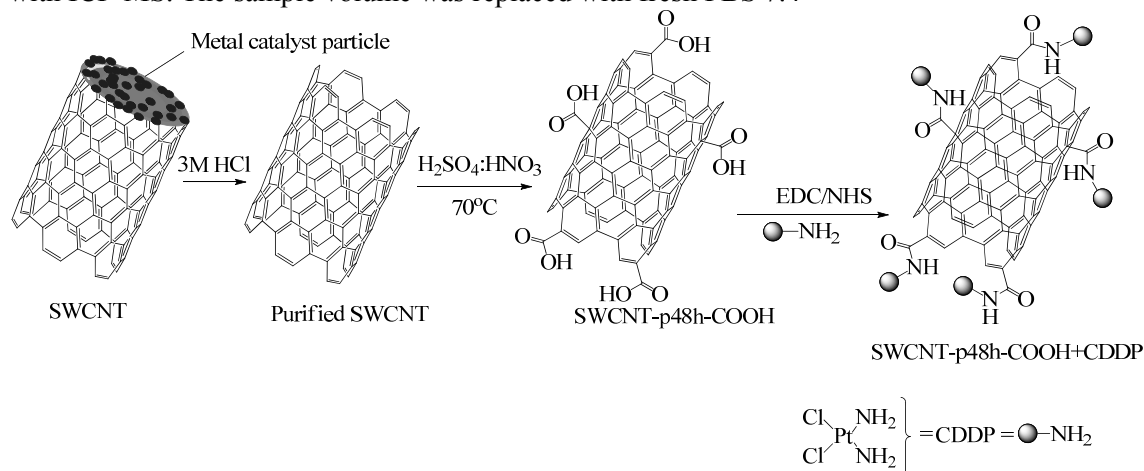


Fig. 1. Scheme of purification, oxidation and activation process of SWCNTs with CDDP

2.3 Advanced characterization

Fourier transform infrared spectroscopy (FTIR) spectra of SWCNTs, purified SWCNTs oxidized SWCNTs and activated SWCNTs with CDDP were registered on a Bruker Vertex 70 equipment in 400 ÷ 4000 cm^{-1} range with 4 cm^{-1} resolution and 32 scans. The samples were analyzed in KBr pellets.

Raman spectra were recorded on a DXR Raman Microscope (Thermo Scientific) by 532 nm laser line. The 10x objective was used to focus the Raman microscope.

Thermogravimetry analysis (TGA) of the samples was done on Q500 TA equipment, using nitrogen atmosphere from 20 °C to 900 °C with 10 °C/min heating rate.

The X-ray photoelectron spectroscopy (XPS) spectra were recorded on Thermo Scientific K-Alpha equipment, fully integrated, with an aluminum anode monochromatic source. Survey scans (0-1350 eV) were performed to identify constitutive elements.

The X-Ray diffraction measurements have been performed on a BRUKER D8 ADVANCE type X-ray diffractometer. The working parameters are 40 kV and 40 mA. The 2 θ scan range was set to 5–50° with a step size of 0.04° and a resolution of 0.01°.

Scanning electron microscopy (SEM) was done on a Quanta Inspect F, a FEI instrument, with a field emission electron gun, 1.2 nm resolution and X-ray energy dispersive spectrometer having an accelerating voltage of 30 kV.

Inductively coupled plasma mass spectrometry (ICP-MS) is an ELAN DRC-e Perkin Elmer SCIEX U.S.A equipment with detection limit of 0.001 $\mu\text{g/g}$.

3. Results and discussion

3.1 FT-IR Spectroscopy

The FT-IR spectrum of SWCNTs-p48h-COOH+CDDP was obtained using the KBr method, thus KBr pellets were obtained having 0.5% concentration of SWCNTs-p48h-COOH+CDDP. Figure 2 presents the FT-IR spectra for SWCNTs, SWCNTs-p48h, SWCNTs-p48h-COOH and SWCNTs-p48h-COOH+CDDP. It can be seen that after oxidation the characteristic peaks corresponding to C=O stretching vibration bonds from carboxylic groups appear at 1715 and 1635 cm^{-1} [17, 18] indicating that COOH functionalization was performed.

According to SWCNTs-p48h-COOH+CDDP structure, spectrum 4 shows the appearance of two new peaks, one at 694 cm^{-1} corresponding to the deformation vibration of NH bonds and the second at 532 cm^{-1} assigned to the HN-Pt stretching vibration [19].

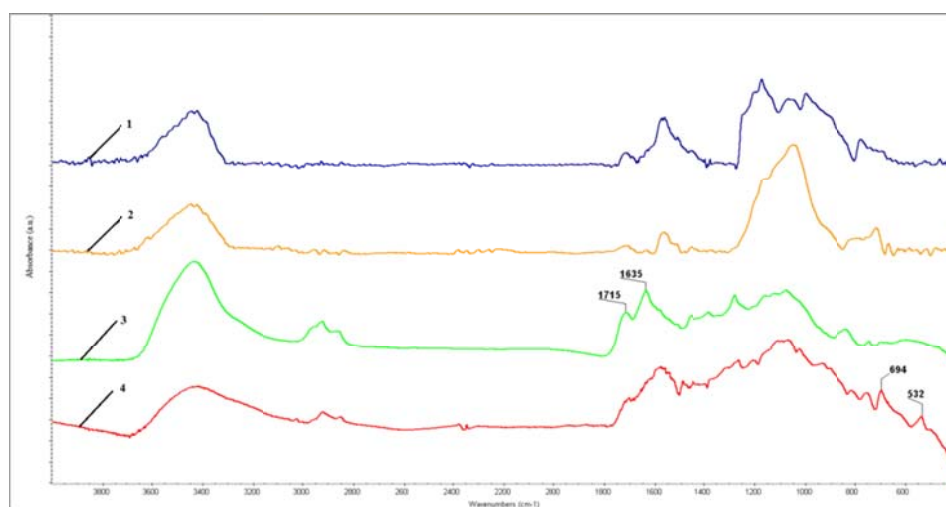


Fig. 2. FT-IR spectra for 1) SWCNTs, 2) SWCNTs-p48h, 3) SWCNTs-p48h-COOH and 4) SWCNTs-p48h-COOH+CDDP

2.2 RAMAN Spectroscopy

Raman spectroscopy was performed to obtain information about the nanocomposites through characteristic D and G peaks from CNT spectra by analyzing the defects that can appear in sp^2 graphitic structure of the nanotubes wall. In order to verify the modification of CNT structure it was calculated the I_D/I_G ratio which gave information about the functionalization reaction.

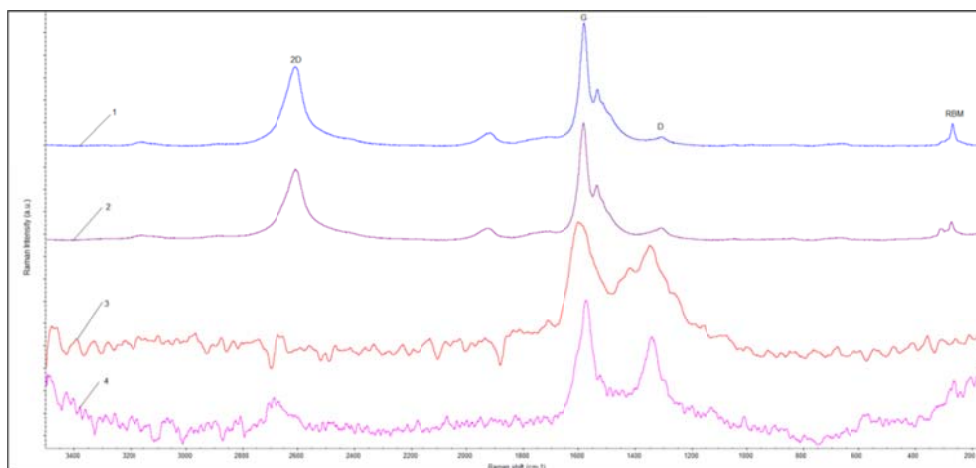


Fig. 3. Raman spectra for 1) SWCNT, 2) SWCNT-p48h, 3) SWCNT-p48h-COOH and 4) SWCNT-p48h-COOH+CDDP

Although purification of SWCNTs did not modified significantly the I_D/I_G ratio value, it was observed that after oxidation (spectrum 3) this value increases from 0.1 to 0.8 meaning that the SWCNTs surface was considerably modified by the introduction of carboxyl groups and possible other structural defects, due to the extreme oxidation conditions. After activation of SWCNT-p48h-COOH with CDDP, the I_D/I_G ratio shows a small decrease which can be explained by the enriched electronic density of CDDP which has small molecules and could be attached also noncovalently on the graphitic wall of CNTs [12] between carboxyl type defect sites.

Table 1. I_D/I_G ratio for SWCNTs, SWCNTs-p48h, SWCNTs-p48h-COOH, SWCNTs-p48h-COOH+CDDP.

Sample	I_D	X_D, cm^{-1}	I_G	X_G, cm^{-1}	I_D/I_G
SWCNT	115.0	1308.3	1556.4	1581.2	0.07
SWCNT-p48h	174.2	1311.0	1679.1	1582.9	0.10
SWCNT-p48h-COOH	226.9	1349.6	284.7	1598.4	0.79
SWCNT-p48h-COOH+CDDP	6.13	1347.8	8.28	1574.4	0.76

2.3 Thermogravimetric analysis

Thermogravimetric analysis (TGA) is a method that gives the information about the thermal stability and the weight loss of nanocomposites by heating the samples from 20 to 900°C in nitrogen atmosphere.

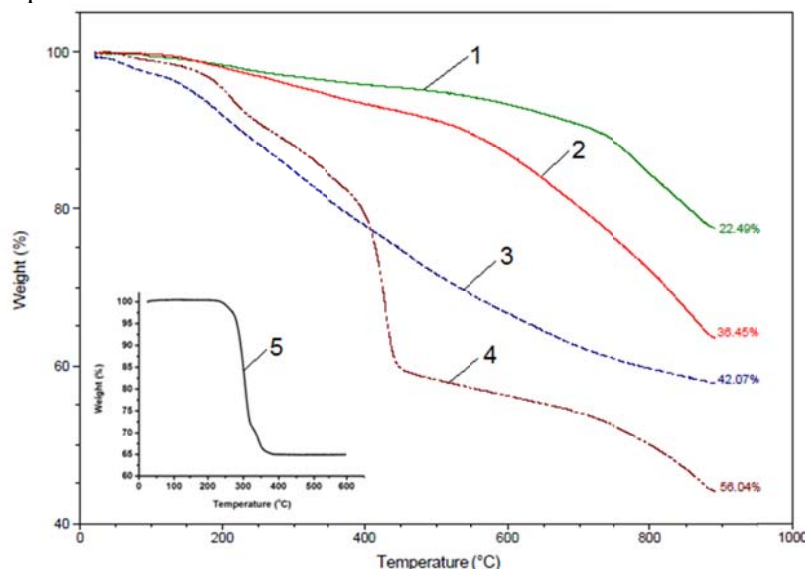


Fig. 4. Thermogravimetric curves for 1) SWCNT, 2) SWCNT-p48h, 3) SWCNT-p48h-COOH, 4) SWCNT-p48h-COOH+CDDP and inset 5) CDDP.

Degradation of SWCNTs-p48h-COOH+CDDP as it can be seen in figure 3 curve 4 presents different behavior compared with SWCNTs-p48h-COOH curve in terms of gradually weight loss. Three main steps are noticed, thus the first stage is attributed to the amino bonds dissociation and the decarboxylation and dehydrogenation processes of $-\text{COOH}$ groups near 200°C, the second stage is assigned to the degradation of CDDP between 350 – 500°C and the third stage corresponds to the degradation of SWCNTs. The total mass loss of SWCNT-p48h-COOH+CDDP is 56% compared with 42% for SWCNTs-p48h-COOH. [14, 15].

2.4 XPS Analysis

The XPS analyses were employed to determine the surface elemental composition of our samples. Thus from figure 5 it can be observed the presence of oxygenated structures through O1s which increase dramatically after oxidation process from 3.78 to 18.97 At.%. This was expected

because the ratio between C atoms and O atoms is modified during oxidation by the introduction of carboxylic groups. Also the activation process was highlighted by the appearance of Pt 4f element which indicates the bonding of CDDP to the SWCNTs surface.

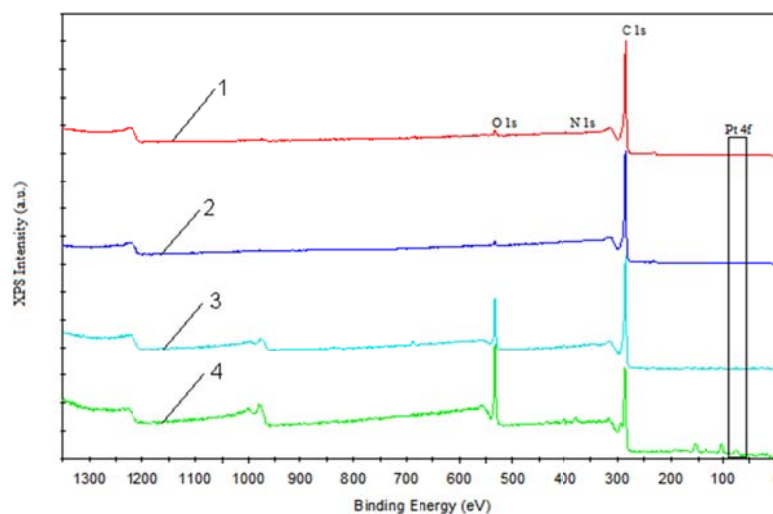


Fig. 5. XPS spectra for 1) SWCNT, 2) SWCNT-p48h, 3) SWCNT-p48h-COOH, 4) SWCNT-p48h-COOH+CDDP

Table 2. XPS data for SWCNTs, SWCNTs-p48h, SWCNTs-p48h-COOH, SWCNTs-p48h-COOH+CDDP

Sample At %	SWCNT	SWCNT- p48h	SWCNT-p48h- COOH	SWCNT-p48h- COOH+CDDP
C 1s	96.43	96.09	81.03	83.4
O 1s	3.25	3.78	18.97	14.16
Mo 3d	0.32	0.13	0	0
N 1s	0	0	0	1.42
Pt 4f	0	0	0	1.02

The values from table 2 show the surface composition of our samples before and after oxidation and respectively CDDP functionalization. The appearance of Pt 4f at 72 eV having 1.02 at % and N 1s from amino and amide groups having 1.42 at % demonstrate the presence of CDDP on SWCNTs surface.

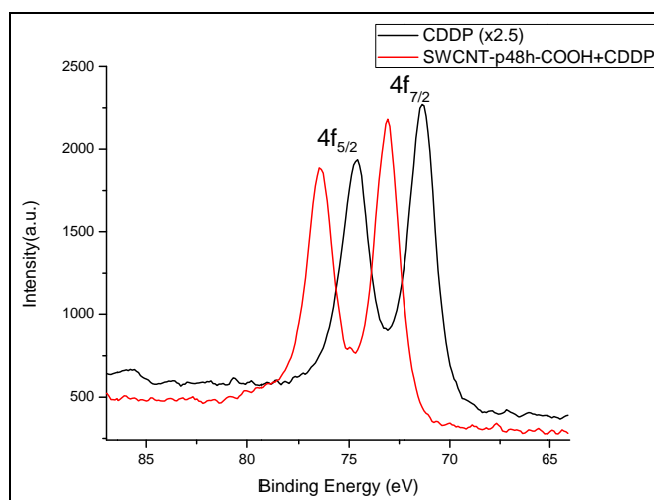


Fig. 6. XPS spectra of Pt 4f element from CDDP and SWCNTs-p48h-COOH+CDDP

Deconvolution of Pt 4f element (Figure 6) from CDDP and SWCNTs-p48h-COOH+CDDP was performed in order to determine the bonding mode of CDDP to SWCNTs and the ratio between the absorption bands of Pt element was calculated.

For SWCNT-p48h-COOH+CDDP the maximum energy of Pt 4f_{5/2} shows a shifting from 74.57 to 76.48 eV and respectively Pt 4f_{7/2} band from 71.36 to 73.09 eV compared with CDDP. By calculating the difference, it results a shifting of 1.91 eV for Pt 4f_{5/2} and 1.73 eV for Pt 4f_{7/2}. Through correlation with the data existing in the literature it was found that the bond between the carboxyl groups from SWCNTs and the amino groups from CDDP is amide type linkage [20].

2.5 X-ray Diffraction

X-ray diffraction was employed to calculate the dimensions of the nanotubes and nanocomposites through Debye-Scheerer equation (2)

$$D = \frac{K * \lambda}{\beta * \cos(\theta)} \quad (2)$$

Where D is the dimension of the nanotubes and nanocomposites form 002 direction, $\lambda=1.54 * 10^{-10}$ m, β is half-width in radian calculated by peak aria from 002 direction and K is constant = 0.9.

Table 3. XRD data for SWCNTs, SWCNTs-p48h, SWCNTs-p48h-COOH, SWCNTs-p48h-COOH+CDDP.

Sample	θ (°)	$\theta/2$ (°)	Cos(θ)	Half-width (°)	Half-width (rad)	Half-width *cos(θ)	D*100 (nm)
SWCNT	25.71	12.85	0.97	2.20	38.37	37.22	3.72
SWCNT-p48h	25.74	12.87	0.97	2.33	40.64	39.42	3.51
SWCNT-p48h-COOH	25.7	12.85	0.97	2.35	40.99	39.76	3.48
SWCNT-p48h-COOH+CDDP	25.7	12.85	0.97	1.7	29.65	28.76	4.81

Structural characterization by XRD data from table 3 show that the dimension of nanotubes decreases after purification and oxidation process due to the removal of amorphous carbon and metal particles from catalyst used for the SWCNTs synthesis. This trend for decrease is correlated with XPS where Mo 3d content was 0 after oxidation process.

After activation process, the dimension of nanocomposites obtained by covalent functionalization of SWCNTs with CDDP increases from 3.48 to 4.81 nm. This increase can be explained by the CDDP bonding onto SWCNTs surface [21].

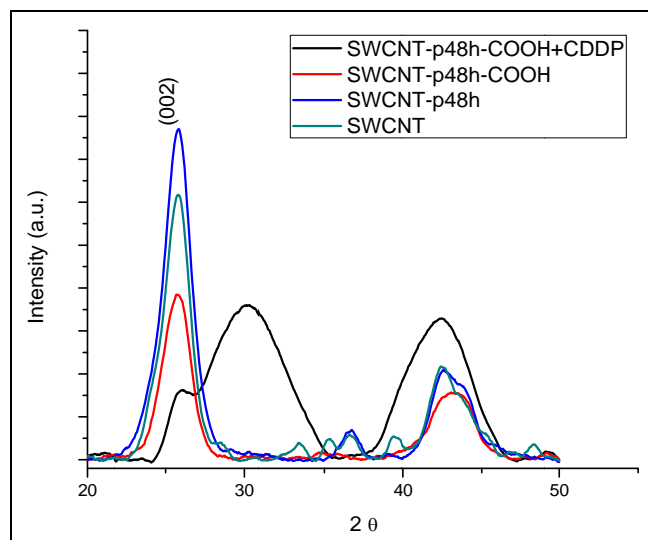


Fig. 7. XRD patterns for SWCNT, SWCNT-p48h, SWCNT-p48h-COOH, SWCNT-p48h-COOH+CDDP

2.6 Scanning electron microscopy

Electronic microscopy of SWCNTs samples was performed on dry powder which could be the cause of their agglomerated appearance; also it can be noticed in Figure 8a that oxidized SWCNTs have clean-cut ends due to higher density of functional groups in that area. When drug loading occur, the bundles are broken (noticeable even in dry state), due to the fact that CDDP molecules hinder Van der Waals forces that manifest usually between CNTs. SEM image from figure 8b shows white points at the end of the SWCNTs which can be considered CDDP bonded to the carboxyl groups from SWCNTs .

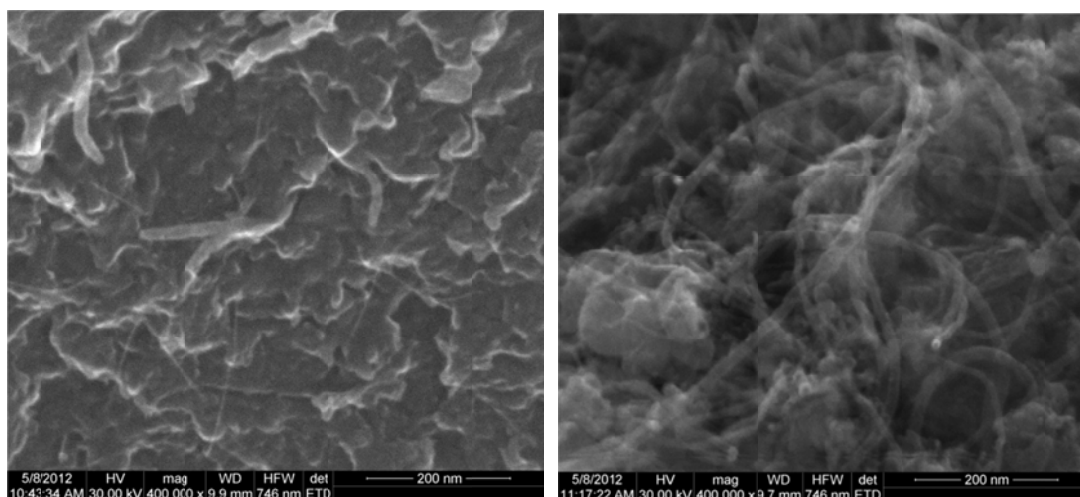


Fig. 8. SEM images for SWCNT-p48h-COOH+CDDP

2.7 Drug delivery study using Inductively coupled plasma mass spectrometry

In order to evaluate the drug release from SWCNTs it was realized the drug release profile using the data given by ICP-MS.

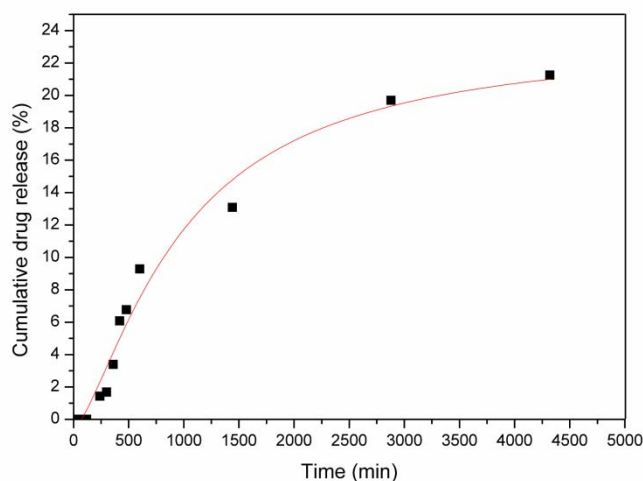


Fig. 9. Drug delivery profile of CDDP from SWCNT-p48h-COOH+CDDP

From figure 9 it can be observed that the CDDP begins to release after 150 minutes releasing 1.2% of drug. After 72 h (4320 minutes) the drug released was 21.3% which is in good agreement with the data reported in the literature [22, 23].

Calculations of the amount of CDDP attached on the SWCNTs surface showed that all the drug quantity was incorporated during nanocomposite synthesis, thus the initial stage of slow release could be explained by the fact that the drug was covalently bonded to the nanotubes and breaking these bonds takes some time given these conditions.

This low release rate can be explained by the impossibility of breaking all C-N bonds in PBS 7.4 formed during the activation reaction [24].

3. Conclusions

This study developed a new route for synthesis of nanocomposites based on covalent functionalization of SWCNTs with CDDP for drug delivery systems. Using XPS and FT-IR characterization it was established that the molecules of CDDP were covalently bonded on SWCNTs functionalized with carboxyl groups.

The XRD patterns proved that the surface of SWCNTs was modified through the increasing of the dimensions for nanocomposites samples. The SEM micrographs showed the presence of CDDP especially on the ends of SWCNTs due to the higher functionalization density in this area.

In vitro drug release from SWCNT-p48h-COOH+CDDP was performed using ICP-MS and it was observed that the content of drug released after 72h was 21%.

Acknowledgement

The work has been funded by the Sectoral Operational Programme Human Resources Development 2007-2013 of the Romanian Ministry of Labour, Family and Social Protection through the Financial Agreement POSDRU/107/1.5/S/76903.

References

- [1] L. Meng, X. Zhang, Q. Lu, Z. Fei, P. J. Dyson, *Biomaterials* **33**, 1689, (2012).
- [2] Z. Liu, J. T. Robinson, S. M. Tabakman, K. Yang, H. Dai, *Mater Today* **14**, 7-8, (2011).

- [3] S. K. Vashist, D. Zheng, G. Pastorin, K. Al-Rubeaan, J. H.T. Luong, F.-S. Sheu, *CARBON* **49**, 4077, (2011).
- [4] S. Prakash, M. Malhotra, W. Shao, C. Tomaro-Duchesneau, S. Abbasi, *Adv Drug Deliver Rev.* **63**, 14-15, (2011).
- [5] X. Zhang, L. Meng, Q. Lu, Z. Fei, P. J. Dyson, *Biomaterials* **30**, 6041 (2009).
- [6] E. Heister, V. Neves, C. Tilmaciu, K. Lipert, V. S. Beltran, H. M. Coley, S. Ravi P. Silva, J. McFadden, *CARBON* **47**, 2152 (2009).
- [7] J.L. Bahr, E.T. Mickelson, M.J. Bronikowski, R.E. Smalley, J.M. Tour, *Chem Commun.* **193**, 4, (2001).
- [8] M Lebron-Colon, M A Meador, D Lukco, F Sola, J Santos-Perez, L S McCorkle, *Nanotechnology* **22**, 45, (2011).
- [9] C. Nichita, I. Stamatina, *Digest Journal of Nanomaterials and Biostructures*, **8**(1), 445, (2013).
- [10] R.P. Feazell, N Nakayama-Ratchford, H. Dai, S.J. Lippard, *J Am Chem Soc.* **129**, 8438, (2007).
- [11] A. Bianco, K. Kastarelos, C.D: Partidos, M Prato, *Chem Commun.* **5**, 571, (2005).
- [12] C. Tripisciano, K. Kraemer, A. Taylor, E. Borowiak-Palen, *CHEM PHYS LETT.* **478**, 200, (2009).
- [13] A.A. Bhirde, A.A. Sousa, V. Patel, A.A. Azari, J.S. Gutkind, R.D. Leapman, J.F. Rusling, *Nanomedicine-UK* **4**, 7, (2009).
- [14] K. Werengowska-Cieciewicz, M. Wisniewski, A. P. Terzyk, N. Gurtowska, J. Olkowska, T. Kloskowski, T. A. Drewna, U. Kiełkowska, S. Druzynski, *CARBON* **70**, 46, (2014).
- [15] J. Li, S. Q. Yap, S. L. Yoong, T. R. Nayak, G. W. Chandra, W. H. Ang, T. Panczyk, S. Ramaprabhu, S. K. Vashist, F.-S. Sheu, A. Tan, G. Pastorin, *CARBON* **50**, 1625 (2012).
- [16] C. C. Ciobotaru, C. M. Damian, H. Iovu, *U.P.B. Sci. Bull. B*, **75**, 2, (2013).
- [17] M. M. Stylianakis, J. A. Mikroyannidis, E. Kymakis, *SOL ENERG MAT SOL C*, **94**, 2, (2010).
- [18] A. Li, L. Wang, M. Li, Z. Xu, P. Li, Z. Z. Zhang, *Digest Journal of Nanomaterials and Biostructures*, **9**(2), 599, (2014).
- [19] S. Likhitar, A. K. Bajpai, *Carbohydr Polym*, **87**, 1, (2012).
- [20] A. Guven, I. A. Rusakova, M. T. Lewis, L. J. Wilson, *Biomaterials* **33**, 1455, (2012).
- [21] K. Ajima, M. Yudasaka, A. Maigne, J. Miyawaki, S. Iijima, *J Phys Chem B* **110**, 5773, (2006).
- [22] H. Xiao, R. Qi, S. Liu, X. Hua, T. Duan, Y. Zhenga, Y. Huang, X. Jing, *Biomaterials* **32**, 7732, (2011).
- [23] S. Bontha, A. V. Kabanov, T. K. Bronich, *J Control Release* **114**, 163, (2006).
- [24] K. Ajima, T. Murakami, Y. Mizoguchi, K. Tsuchida, T. Ichihashi, S. Iijima, M. Yudasaka, *ACS NANO*, **2**, 10, (2008)